



Synthesis of ferrofluids using a chemically induced transition method and their characterization

Xiangshen Meng¹ · Xiaoyan Qiu¹ · Jianwei Zhao¹ · Yueqiang Lin¹ · Xiaodong Liu¹ · Decai Li² · Jian Li¹ · Zhenghong He¹

Received: 29 August 2018 / Revised: 30 November 2018 / Accepted: 14 December 2018 / Published online: 6 January 2019
© Springer-Verlag GmbH Germany, part of Springer Nature 2019

Abstract

Using an altering chemically induced transition route, magnetic nanoparticles as well as nanoparticles modified with oleic acid have been prepared. The modified nanoparticles have been used to synthesize a high-quality kerosene-based ferrofluid, in which the mass fraction percentage of particles consisting of a γ -Fe₂O₃ core and an oleic acid coating, ϕ_m , amounted to 55%. Ferrofluids having lower concentrations of particles were obtained by diluting the mother ferrofluid. Magnetization measurements showed the as-synthesized ferrofluids to have excellent dispersity of the particles and field-induced inter-particle interactions. Optical transparency measurements confirmed that the ferrofluids showed a sensitive field-induced effect of chain-like aggregation, with redispersion of the particles after removing the magnetic field. According to results concerning both particle structure and ferrofluid density, the volume fraction percentage of particles, including both the γ -Fe₂O₃ core and the oleic acid coating, ϕ'_v , as well as that of the γ -Fe₂O₃ alone, ϕ_v , can be deduced.

Keywords Ferrofluids · Synthesis · Characterization

Introduction

Magnetic nanoparticles in the size range 1–100 nm represent an important class of artificial nanostructured materials and have attracted increasing interest in relation to fundamental science and technological applications [1–5]. One application of magnetic nanoparticles is to prepare ferrofluids, which are stable colloidal dispersions of nanosized ferro- or ferrimagnetic particles suspended in a liquid carrier, thereby constituting a magnetic functional material with fluidity. The size of magnetic particles in ferrofluids must be sufficiently small, since the stability of a ferrofluid as a colloidal system is ensured by thermal motion of the particles. At the same time, particles

must not be too small, since if the size is less than 1–2 nm, their magnetic properties disappear [6]. Generally, the size of the magnetic particles is 10 nm or so. Due to the strong magnetic dipole–dipole interactions between magnetic nanoparticles, as well as their high surface energy, magnetic nanoparticles tend to spontaneously agglomerate. To prevent this, they are stabilized by coating with long-chain molecular polymer/surfactant or by electrostatic repulsion. Correspondingly, ferrofluids can be divided into those that are surfactant ones and those that are ionic (electrostatic double-layer) ones [7, 8]. By applying an external magnetic field, some behaviors of ferrofluids, such as optical properties and viscosity [9], can be changed, which are referred to as field-induced effects. For the synthesis of ferrofluids, the most commonly used and chemically stable ferrites are magnetite (Fe₃O₄) and maghemite (γ -Fe₂O₃) [10]. For optical behavior, that is, magneto-optical effects, persistent Fe²⁺ needs to be prevented in order to improve the transparency of the ferrite particles [11, 12]. Hence, γ -Fe₂O₃ nanoparticles may be more suitable than Fe₃O₄ nanoparticles for synthesizing ferrofluids showing pronounced magneto-optical effects, even though the magnetization of the former is less than that of the latter.

The field-induced effects of ferrofluids result from a microstructure transition. For formation of clusters, the dipole–dipole

✉ Jian Li
aizhong@swu.edu.cn

✉ Zhenghong He
Hezhhenho@swu.edu.cn

¹ School of Physical Science and Technology, Southwest University, Chongqing 400715, China

² State Key Laboratory of Tribology, Tsinghua University, Beijing 100084, China

energy of the particles has to overcome the thermal energy [13]. In the absence of a magnetic field, the magnetic nanoparticles in ferrofluids are in a random state of thermal motion. When an external magnetic field is applied, the magnetic moments fixed inside the particles favor the field's direction and the interparticle interaction will be enhanced. Consequently, the particles can form chain-like aggregates of head-to-tail linked moments along the field's direction, which strongly affect the macroscopic properties of the systems and thus lead to many potential applications. Hence, the dispersity of the particles in a ferrofluid before and after applying a magnetic field is a very important characteristic. Generally, electron microscopy offers a direct method for nanostructure observation. However, for investigation of the structure of ferrofluids, only information about the size of separate particles can be obtained, because the structure would undergo uncontrollable change during sample preparation prior to examination [14]. The saturation magnetization relationship between a ferrofluid and magnetic nanoparticles can be expressed as $M_{fs} = \phi_v M_{ps}$, where M_{fs} and M_{ps} are the saturation magnetizations of the ferrofluid and nanoparticles, respectively, and ϕ_v is the volume fraction of particles in the ferrofluid. Experiments have shown that, due to self-assembled aggregates of ring-like micelle structures, M_{fs} may be less than $\phi_v M_{ps}$ [15, 16]. Consequently, the dispersity of the nanoparticles in ferrofluids can be revealed by magnetization measurements. Moreover, magneto-optical effects are not only critical for technological applications but also provide useful tools to probe the microstructural properties of ferrofluids [17, 18]. In a gradient magnetic field, chain-like aggregates will form and move, such that the variation of the light intensity transmitted through a ferrofluid film can behave as a relaxation process arising from the “geometric shadowing effect” [19, 20]. After removal of the field, the aggregates will break and the transmitted light will change accordingly. Thus, the behavior of the transmitted light is also a useful tool for probing field-induced aggregation in a ferrofluid.

Most studies of magnetic nanoparticles have focused on the development of novel synthetic methods [21, 22]. Different syntheses produce iron oxide materials with different external magnetic properties [23]. We previously proposed a method for preparing γ - Fe_2O_3 nanoparticles coated with FeCl_3 by treating an $\text{FeOOH/Mg}(\text{OH})_2$ precursor with a solution of FeCl_2 , which is known as a chemically induced transition (CIT) [24, 25]. Experimental results have shown that such magnetic nanoparticles are suitable for directly synthesizing ionic ferrofluids [26]. Furthermore, surface modification with oleic acid has been attempted for the nanoparticles coated with FeCl_3 . Experiments have shown that the as-prepared samples are a mixture of both γ - $\text{Fe}_2\text{O}_3/\text{FeCl}_3 \cdot 6\text{H}_2\text{O}$ and γ - Fe_2O_3 /oleic acid nanoparticles when the amount of oleic acid added is not sufficient [27]. In the present work, we have developed a CIT method for the preparation of γ - Fe_2O_3 nanoparticles with no FeCl_3 coating for use in surface-modified ferrofluids. The

microstructures of both the as-prepared nanoparticles and the ferrofluid have been characterized.

Experimental results and analysis

Preparation of the nanoparticles

Generally, synthesis processes for ferrofluids can be divided into two steps, namely preparation of the particles, followed by their dispersal to form a stable colloidal solution [28]. A general scheme for preparing magnetic nanoparticles by the CIT method used here is shown in Fig. 1. The $\text{FeOOH/Mg}(\text{OH})_2$ precursor was prepared by a co-precipitation method, details of which have been reported elsewhere [29]. The precursor (10 g) was mixed with water (250 mL). This mixture and

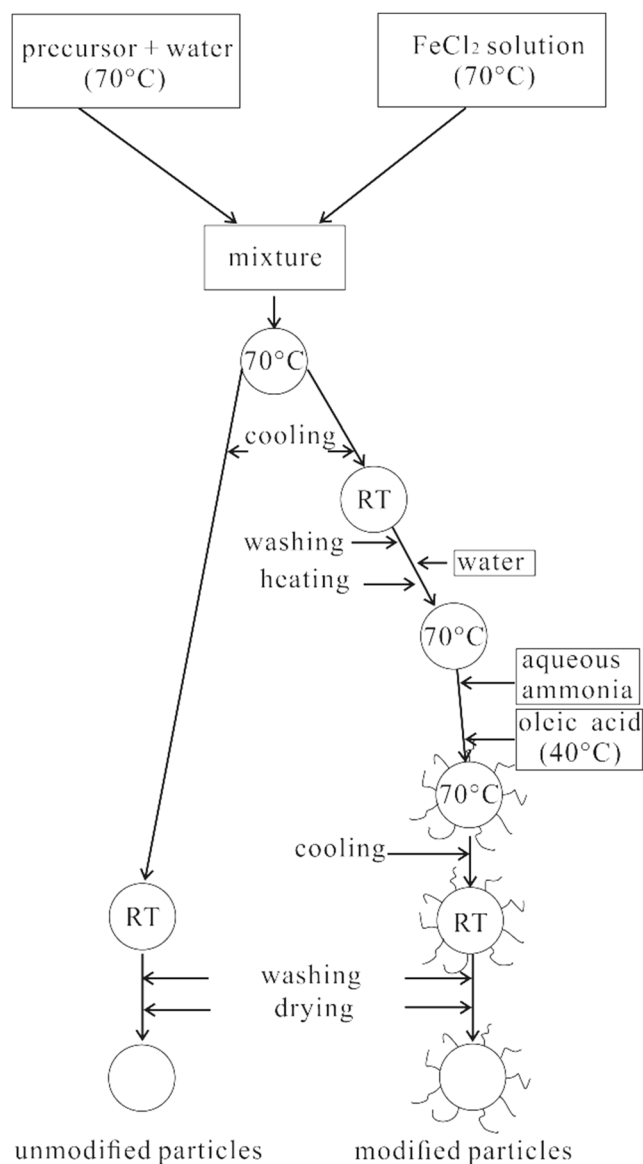


Fig. 1 Preparation scheme for magnetic nanoparticles by the CIT method

a FeCl_2 solution (0.06 M, 400 mL) were each heated to 70 °C. They were then combined, and the mixture was kept at 70 °C and stirred under reflux for 30 min to assist the chemically induced transition. Heating was then stopped, whereupon the product was gradually precipitated. By washing and drying, bare nanoparticles without an oleic acid coating were obtained. These constituted a contrast sample having no oleic acid and were designated as unmodified sample/unmodified particles.

For oleic acid surface modification, the sluggish product after washing was taken up in water (390 mL). After heating to 70 °C, aqueous ammonia (25%, 10 mL) was added to form an alkaline solution, and then oleic acid (6 mL, 40 °C) was added. The resulting mixture was kept at 70 °C for 40 min. After cooling to room temperature (RT), washing, and drying, nanoparticles modified with oleic acid were obtained, which are designated as modified sample/modified particles.

Structure of the as-prepared particles

Energy-dispersive X-ray spectroscopy (EDS) measurements, as shown in Fig. 2, confirmed that the unmodified sample contained O and Fe, whereas the modified sample contained O, Fe, and C. Quantitative results in terms of atomic percentages are shown in Table 1. For the particles modified with oleic acid, using the atomic percentages of Fe and C, a_{Fe} and a_{C} , determined by EDS, the molar percentage of $\gamma\text{-Fe}_2\text{O}_3$, y_γ , and that of oleic acid ($\text{C}_{18}\text{H}_{34}\text{O}_2$), y_o , could be estimated from the following equation:

$$y_\gamma = \frac{a_{\text{Fe}}/2}{a_{\text{Fe}}/2 + a_{\text{C}}/18} \times 100, \quad y_o = 100 - y_\gamma \quad (1)$$

The mass fraction percentages of $\gamma\text{-Fe}_2\text{O}_3$ and oleic acid, z_γ and z_o , could then be deduced from:

$$z_\gamma = \frac{y_\gamma A_\gamma}{y_\gamma A_\gamma + y_o A_o} \times 100, \quad z_o = 100 - z_\gamma \quad (2)$$

where A_γ and A_o are the molar masses of $\gamma\text{-Fe}_2\text{O}_3$ and oleic acid, respectively. The results calculated from Eqs. (1) and (2) are also listed in Table 1.

Fig. 2 EDS spectra of (a) the unmodified sample and (b) the modified sample. The insets are of specific zones

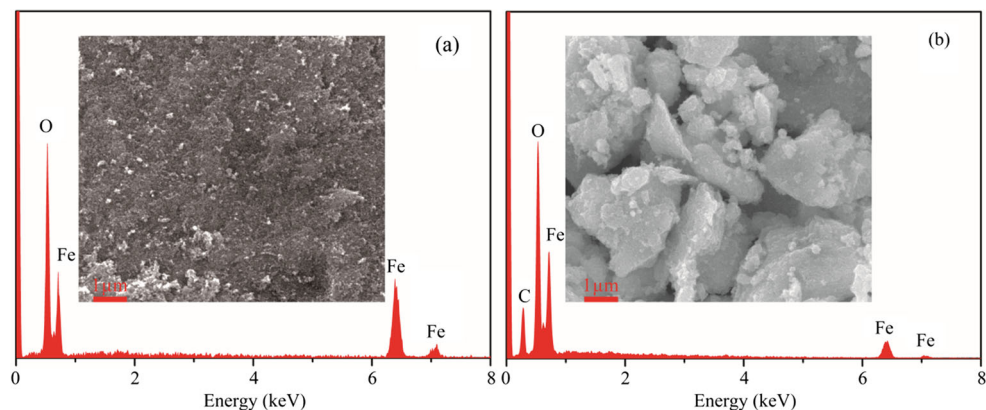


Table 1 Atom fraction percentages (a_i) measured by EDS for the unmodified and modified samples, and molar fraction percentages (y_i) and mass fraction percentages (z_i) of each phase for the modified sample

Particles	O	Fe	C	y_γ/y_o	z_γ/z_o
Unmodified	67.26	32.74	0		
Modified	49.96	25.40	27.64	89.21/10.79	82.38/17.62

X-ray diffraction (XRD) patterns, as shown in Fig. 3, indicated that both the bare and modified samples consisted predominantly of maghemite ($\gamma\text{-Fe}_2\text{O}_3$, JCPDS no.39-1346). For the ferrite, the grain size d_c could be estimated from the (311) peak in the XRD pattern using the Scherrer equation [30]:

$$d_c = \frac{k\lambda}{\beta \cos\theta} \quad (3)$$

where k is a constant ($k=0.89$), λ is the X-ray wavelength ($\text{Cu-K}\alpha = 0.1542 \text{ nm}$), θ is the Bragg diffraction angle of the (311) plane, and β is the full-width at half-maximum of the (311) diffraction peak. For the bare and modified samples, the d_c values obtained were 11.5 and 12.0 nm, respectively.

Transmission electron microscopy (TEM) observation showed that the unmodified sample was composed of approximately spherical nanoparticles, whereas the modified sample also contained some flaked particles. Typical TEM images for the bare and modified particles are illustrated as the insets in Fig. 3.

Assuming a close-packed monolayer of the surfactant on the surface of a nanoparticle of diameter x , the mass of the surface monolayer is $m_s = (\pi x^2/a)(M/N_0)$ and the mass of the particle core is $m_c = \pi x^3 \rho/6$, where a is the head area per molecule of the surfactant, M is the molar mass of the surfactant, N_0 is Avogadro's number, and ρ is the density of the particle core [31]. Accordingly, the mass fraction percentage of the surfactant z_s can be expressed as:

$$z_s = \frac{m_s}{m_s + m_c} \times 100 \quad (4)$$

For the sample modified with oleic acid, the particles appear spherical, and their size x can be approximated

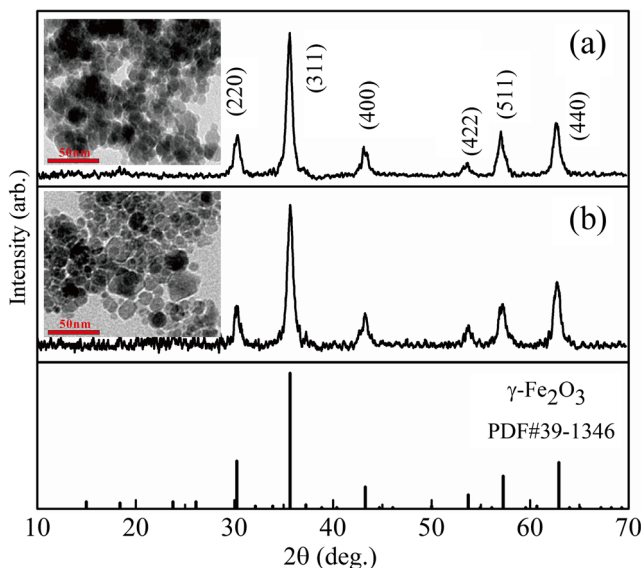


Fig. 3 XRD patterns of (a) the unmodified sample and (b) the modified sample. The insets show typical TEM images

as the grain size d_c . Thus, using a (22×10^{-16} cm²/mol) [32] and M for oleic acid (282.452 g/mol) and the density ρ of γ -Fe₂O₃ (4.90 g/cm³), the z_s value of the modified sample was evaluated as 17.87. The theoretically estimated z_s value is clearly in good agreement with the experimentally determined mass fraction percentage of oleic acid z_o (= 17.62). This result shows that the modified particles were coated with a monolayer of oleic acid, making them suitable for preparing an oil-based ferrofluid [33].

From the mass fraction percentages of γ -Fe₂O₃ and oleic acid, z_γ and z_o , measured by EDS, the average density of the nanoparticles in the modified sample, $\langle \rho_p \rangle$, can be written as:

$$\langle \rho_p \rangle = \frac{\rho_\gamma \rho_o}{z_\gamma \rho_o + z_o \rho_\gamma} \times 100 \quad (5)$$

where ρ_γ and ρ_o are the densities of γ -Fe₂O₃ and oleic acid, respectively. From the measured z_γ and z_c values and the densities of both γ -Fe₂O₃ and oleic acid (0.893 g/cm³), $\langle \rho_p \rangle$ was evaluated as 2.74 g/cm³.

Preparation of ferrofluids

To prepare ferrofluids, the modified particles were added to kerosene in a ratio of 15 g to 10 mL. The mixture was heated to 110 °C and stirred under reflux for 30 min. After cooling to room temperature, the mixture was centrifuged at 4.5×10^3 rpm for 5 min to obtain a stable mother ferrofluid [34].

Using a density meter, the density of the mother ferrofluid, ρ_f , was determined as 1.3084 g/mL. Thus, the mass fraction

percentage of modified particles in the ferrofluid, ϕ_m , can be expressed as:

$$\phi_m = \frac{m_p}{m_p + m_c} \times 100 = \frac{\langle \rho_p \rangle}{\rho_f} \left(\frac{\rho_f - \rho_c}{\langle \rho_p \rangle - \rho_c} \right) \times 100 \quad (6)$$

where m_p and m_c are the mass of the γ -Fe₂O₃ particles coated by oleic acid and the kerosene carrier liquid, respectively, and ρ_c is the density of the kerosene (0.8 g/mL). Accordingly, the mass fraction percentage of the mother ferrofluid was evaluated as 55.0%. The ferrofluid showed good stability, with no phase separation after 6 months. A high-quality ferrofluid should develop spikes on its surface when it is brought into contact with a moderate magnetic field [33, 35, 36]. A micrographic spike pattern for the as-synthesized mother ferrofluid was clearly seen, as shown in Fig. 4. TEM observation revealed that the ferrofluid particles were approximately spherical (inset (1) in Fig. 5 (a)), and a high-resolution TEM image of a particle shows the particle being a single crystallite (inset (2) in Fig. 5 (a)). In the TEM image, the sizes correspond to γ -Fe₂O₃ core because the oleic acid coating is not visible [37]. Statistical analysis [38] showed that the size of the ferrofluid particles fitted a log-normal distribution:

$$f_{dis}(\ln x) = \frac{1}{\sqrt{2\pi} \ln \sigma_g} \exp \left[-\frac{(\ln x - \ln x_g)^2}{2 \ln^2 \sigma_g} \right], \quad (7)$$

where x_g is the median size and $\ln \sigma_g$ is the standard deviation, evaluated as 9.73 nm and 0.23, respectively. The average diameter $\langle d \rangle$ can be expressed as:

$$\langle d \rangle = \int_{-\infty}^{\infty} x f_{dis}(\ln x) d \ln x \quad (8)$$

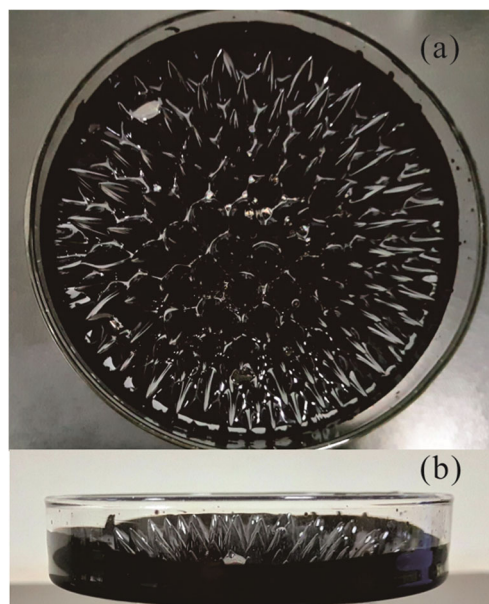


Fig. 4 Top (a) and side (b) views of the spike pattern of the as-synthesized mother ferrofluid

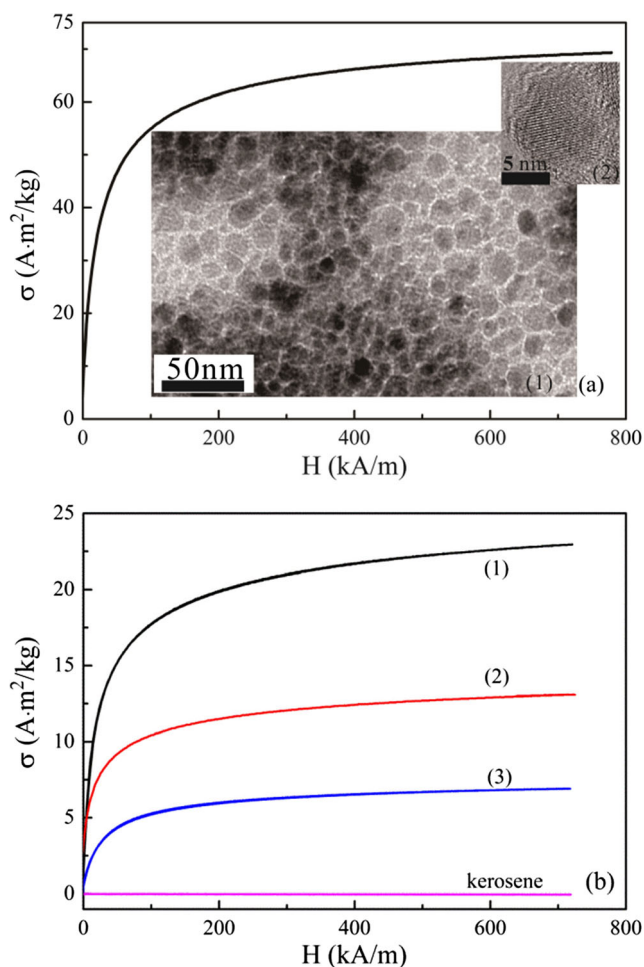


Fig. 5 Specific magnetization curves of (a) the modified particles and (b) the kerosene carrier liquid, as well as of ferrofluid samples (1), (2), and (3). The inset (1) shows a typical TEM image of the ferrofluid particles and the inset (2) shows a high-resolution TEM image of a particle

Consequently, $\langle d \rangle$ was evaluated as 10.00 nm, which is less than the grain size of the modified particles. This result implies that flaked and large particles were removed by the centrifugation treatment.

For magnetization and optical measurements and to characterize the microstructure, ferrofluids with high, medium, and low particle concentrations were prepared by diluting the mother ferrofluid with the kerosene carrier liquid, and these were designated as ferrofluid samples (1), (2), and (3), respectively. The densities of ferrofluid samples (1), (2), and (3) were measured, and the results are listed in Table 2. Using Eq. (6), values of ϕ_m were determined, and these are also listed in Table 2.

Magnetization behavior of the ferrofluids

The specific magnetization curves of σ vs. H for the modified particles, the ferrofluids, and the kerosene carrier liquid were

Table 2 Densities ρ_f , mass fraction percentages of the particles ϕ_m , specific saturation magnetizations $\sigma_{f,s}$, and the reduced specific saturation magnetizations $\sigma'_{f,s}$ for ferrofluid samples (1), (2), and (3)

Ferrofluids	ρ_f (g/mL)	ϕ_m (%)	$\sigma_{f,s}$ (A m ² /kg)	$\sigma'_{f,s}$ (A m ² /kg)
(1)	1.0500	33.63	23.00	68.39
(2)	0.9205	18.48	13.00	70.35
(3)	0.8615	10.08	7.10	70.44

measured by means of a vibrating sample magnetometer (VSM), and the results are shown in Fig. 5. Clearly, the magnetization of the carrier liquid was very weak and could be neglected for the ferrofluids. Specific saturation magnetization (moments of unit mass), σ_s , could be deduced from the relationship of σ vs. $1/H$ under high magnetic field [39]. Accordingly, the specific saturation magnetization of the modified particles, $\sigma_{p,s}$, was evaluated as 71.5 A m²/kg, and those of the ferrofluids with different particle concentrations were as listed in Table 2. For a ferrofluid, the reduced specific saturation magnetization, $\sigma'_{f,s}$, is defined as:

$$\sigma'_{f,s} = \sigma_{f,s} / \phi_m \quad (9)$$

From the values of $\sigma_{f,s}$ and ϕ_m listed in Table 2, $\sigma'_{f,s}$ was calculated for samples (1), (2), and (3), and the results are also listed in Table 2. It can be seen that $\sigma'_{f,s}$ for each sample was approximately 70.0 A m²/kg, consistent with the specific saturation magnetization of the modified particles $\sigma_{p,s}$. This indicates that there is no closed magnetic flux's aggregation in the as-synthesized ferrofluids, because the closed magnetic flux's aggregation does not contribute to the magnetization of the ferrofluid system [12, 40].

Ignoring any inter-particle magnetic interaction and considering the size distribution of the particles, $f_{dis}(\ln x)$, the reduced specific magnetization of a ferrofluid, $\sigma'_f (= \sigma_f / \phi_m)$, can be described by the Langevin equation for a paramagnetic system [38]:

$$\sigma'_f = \sigma_{p,s} \int_{-\infty}^{\infty} L(\alpha) f_{dis}(\ln x) d \ln x \quad (10)$$

Here, $L(\alpha) = \coth \alpha - 1/\alpha$ is the so-called Langevin function, where $\alpha = \mu_0 \tau x^3 \sigma_{p,s} \langle \rho_p \rangle H / 6 k_B T$ is the Langevin parameter, and μ_0 is the magnetic permeability in vacuum, k_B is the Boltzmann constant, and T is the absolute temperature. Taking $T = 290$ K (room temperature), the reduced Langevin theoretical specific magnetization curve, σ'_f vs. H , can be drawn, as shown in Fig. 6. It can be seen from Fig. 6 that the experimentally measured magnetization is clearly higher than the theoretical value in the low-field region, although they are identical in the high-field region. The deviation in the low-field region can be attributed to magnetic interaction between the ferrofluid particles, whereby their magnetic moments are more easily aligned. Consequently, the experimental gradients exceed that of the theoretical curve in the low-

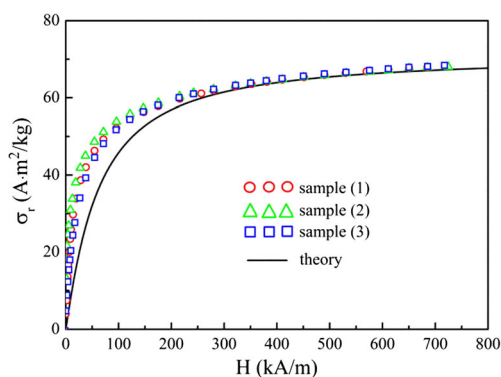


Fig. 6 Theoretical and experimental specific magnetizations reduced by ϕ_m for ferrofluid samples (1), (2), and (3)

field region [41]. With increasing field strength, the moments of the particles tend to orient with the field direction, and the experimental results approach the theoretical curve.

Optical transparency of the ferrofluids

To measure the optical transparency of the ferrofluids, samples were injected into a glass cell of thickness 0.15 mm to form a film. A He–Ne laser was used as the light source and the light beam direction was perpendicular to the film and parallel to the magnetic field generated by an electromagnet. The main details of the experimental device have been described previously [42]. Using a computer equipped with LabVIEW software, the field was controlled by adjusting the electric current, and the light signals were acquired and processed. In the present experiment, the central magnetic field was 300 Oe and the field gradient was about 30 Oe mm⁻¹. The variation in the relative transmitted light intensity T_r with time t was measured, which was used to characterize the optical transparency. T_r is defined as:

$$T_r = I/I_0 \quad (11)$$

where I and I_0 are the intensity of transmitted light after and before application of the magnetic field, respectively.

Figure 7 shows the variation of T_r with time t for ferrofluid samples (1), (2), and (3) with different ϕ_m , whereby the field was applied at $t=0$ and removed at $t=190$ s. It can be seen from Fig. 7 that under the applied magnetic field, the light transmitted through the ferrofluid samples showed optical relaxation behavior similar to that of other ferrofluids [17, 19, 43, 44]. According to Li's theory [44–46], such behavior reflects a process of microstructure transition in ferrofluids, involving the formation of chains from dispersed particles by magnetic interaction, and the motion of these chains due to “magnetic convergent force” and “magnetic divergent force” in the film under the applied magnetic field. Before application of the magnetic field, the magnetic nanoparticles in the ferrofluid film were in a random state of thermal motion, so the intensity of the

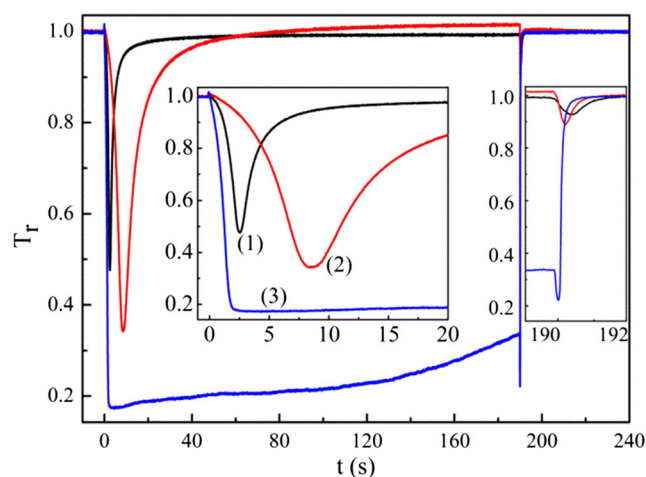


Fig. 7 T_r vs. t curves for ferrofluid samples (1), (2), and (3)

transmitted light was stable. After removing the field, the opposing electrodynamic potential instantaneously enhanced the field strength, and the intensity of the transmitted decreased sharply. The particle chains then dispersed and broke up as the magnetic field decreased to zero, so that the transmitted light reverted to a stable level. From the experimental results shown in Fig. 7, it is clear that the stable levels of transmitted light before and after applying the magnetic field were the same for ferrofluid samples with different ϕ_m . Hence, we surmise that the dispersion behavior of the particle systems after removing the field was the same as that before applying the field. These results concerning optical transparency imply that the as-synthesized ferrofluids not only show sensitive field-response behavior but also excellent post-field replication behavior.

Discussion

EDS results revealed that the unmodified nanoparticles did not contain Cl, in contrast to particles prepared in previous work [24–27]. This could be attributed to heated precursor (70 °C) being mixed with hot FeCl₂ solution (70 °C) in the present work, whereas cold precursor (room temperature) was added to the hot solution in previous work. Therefore, we surmise that by using the thermal mixing route, in which both the precursor and treatment solution are pre-heated, pure γ -Fe₂O₃ nanoparticles can be prepared by the CIT method.

XRD and TEM results indicated that, compared with the unmodified sample, the sample modified with oleic acid had a larger grain size, and contained flake particles, besides sphere-like particles. This suggested that aggregation growth took place during the modification process, which might be ascribed to the high pH of the solution [47, 48] due to the added aqueous ammonia.

Both the magnetization behavior and the optical transparency revealed that the ferrofluids showed good dispersity in the absence of a magnetic field and sensitive field-induced effects.

For ferrofluids, the magnitude of field-induced physical effects is related to the concentration of particles, which is generally expressed by their volume fraction [49]. The typical volume fraction of suspended magnetic materials is a few percent [36, 50]. In addition to the magnetic particles and the carrier liquid, the third essential ingredient of a colloidal ferrofluid is the presence of an adsorbed long-chain molecular species on the particles' surface that prevents agglomeration of the particles to each other [51]. In practice, the volume of the particles is too difficult to determine directly, so the mass fraction percentage, including the magnetic material and the surfactant, ϕ_m , is used in preparing ferrofluids. Correspondingly, the volume fraction percentage, including both the magnetic material and surfactant, ϕ'_v , can be determined from:

$$\phi'_v = \frac{V'_p}{V' + V_c} \times 100 = \frac{\rho_f}{\rho_p} \phi_m \quad (12)$$

where $V'_p (=V_p+V_o)$ is the volume of the surfactant-coated nanoparticles including that of γ -Fe₂O₃ magnetic core (V_p) and oleic acid coating (V_o), V_c is the volume of the carrier liquid, ρ_f and ρ_p are the densities of the ferrofluid and the surfactant-coated nanoparticles, respectively. In Eq. (12), taking the average density of modified particles $\langle \rho_p \rangle$ (2.74 g/cm³) as ρ_p , the volume fraction percentage of the particles, including both the γ -Fe₂O₃ magnetic core and the oleic acid coating, ϕ'_v , can be deduced. The ϕ'_v of the mother ferrofluid was evaluated as 26.20%, and those of the diluted samples (1), (2), and (3) are listed in Table 3.

The saturation magnetization (moments of unit volume) for a ferrofluid, $M_{f,s}$, can be expressed as:

$$M_{f,s} = \rho_f \cdot \sigma_{f,s} \quad (13)$$

The reduced saturation magnetization, $M'_{f,s}$, is given by:

$$M'_{f,s} = M_{f,s} / \phi'_v \quad (14)$$

Values of both $M_{f,s}$ and $M'_{f,s}$ are listed in Table 3. The reduced saturation magnetization values for the ferrofluids with different ϕ'_v are each about 192 kA m⁻¹. Moreover, the

Table 3 Volume fraction percentages of the particles consisting of γ -Fe₂O₃ magnetic cores and oleic acid coating, ϕ'_v , and those consisting only of the magnetic core, ϕ_v , saturation magnetizations, $M_{f,s}$, and the reduced saturation magnetizations, $M'_{f,s}$, for ferrofluid samples (1), (2), and (3)

Ferrofluids	ϕ'_v (%)	ϕ_v (%)	$M_{f,s}$ (kA m ⁻¹)	$M'_{f,s}$ (kA m ⁻¹)
(1)	12.89	6.96	24.15	187.35
(2)	6.21	3.35	11.97	192.75
(3)	3.17	1.71	6.20	195.58

saturation magnetization of the modified particles, $M_{p,s}$, can be obtained by:

$$M_{p,s} = \langle \rho_p \rangle \cdot \sigma_{p,s} \quad (15)$$

From the measured $\sigma_{p,s}$ and average density of the modified particles $\langle \rho_p \rangle$, $M_{p,s}$ was evaluated as 196 kA m⁻¹. $M'_{f,s}$ and $M_{p,s}$ are clearly very similar, which is consistent with the result that having no aggregates of the closed magnetic flux in the ferrofluids, so ϕ'_v can be obtained for ferrofluid samples.

For a ferrofluid, the volume fraction percentage of the magnetic material alone can be written as:

$$\phi_v = \frac{V_p}{V_p + V_o + V_c} \times 100 = \phi'_v \cdot f_m \quad (16)$$

where f_m is the volume fraction of the magnetic phase in the nanoparticles coated with the surfactant. For the modified particles composed of a γ -Fe₂O₃ magnetic core coated with oleic acid, f_m is the volume fraction of the γ -Fe₂O₃ magnetic phase, f_γ , which can be determined from the mass fraction and density of each phase, i.e.:

$$f_m = f_\gamma = \frac{z_\gamma / \rho_\gamma}{z_\gamma / \rho_\gamma + z_o / \rho_o} \quad (17)$$

where z_γ and z_o are the mass fractions of γ -Fe₂O₃ and oleic acid, as listed in Table 1, and ρ_γ and ρ_o are the densities of γ -Fe₂O₃ and oleic acid, respectively. Accordingly, f_γ was obtained as 0.54 and ϕ_v of the mother ferrofluid was evaluated as 12%. Those of the ferrofluid samples (1), (2), and (3) are listed in Table 3.

The above discussion shows that the volume fraction percentage of magnetic material in a ferrofluid, ϕ_v , can be determined from the mass fraction percentage of the composite particles, ϕ_m , and the average density $\langle \rho_p \rangle$ of the composite particles as well as the volume fraction of the magnetic material in the particles f_m . Therefore, in practice, ϕ_m can be designed for the acquired ϕ_v in a ferrofluid, according to the expression:

$$\phi_m = \frac{\phi_v \langle \rho_p \rangle}{\phi_v \langle \rho_p \rangle + (100f_m - \phi_v)\rho_c} \times 100 \quad (18)$$

Generally, the particle concentration will decrease after centrifugation, and so, Eq. (18) should be multiplied by a so-called effective factor F . In the present work, the F factor is 1.18.

Conclusion

By hot mixing of pre-heated FeOOH/Mg(OH)₂ precursor and FeCl₂ solutions, pure γ -Fe₂O₃ nanoparticles without an FeCl₃

coating can be prepared by the CIT method. The pure nanoparticles could be more suitable for the surface modification than the nanoparticles coated with FeCl_3 . The surface of such nanoparticles can be modified with oleic acid to form $\gamma\text{-Fe}_2\text{O}_3$ coated with a monolayer of oleic acid, i.e., $\gamma\text{-Fe}_2\text{O}_3$ /oleic acid composite nanoparticles. Experiments have shown that, during the modification process, the particles may exhibit aggregation growth to produce some flaked particles. This may be attributed to the added aqueous ammonia increasing the pH of the solution.

Based on such $\gamma\text{-Fe}_2\text{O}_3$ /oleic acid composite nanoparticles, high-quality ferrofluids with kerosene as the carrier liquid have been synthesized, in which the average particle size is 10 nm and the mass fraction percentage of $\gamma\text{-Fe}_2\text{O}_3$ /oleic acid composite nanoparticles, ϕ_m , is 55%. Magnetization and optical transparency measurements have revealed that the as-synthesized ferrofluids show excellent dispersity of the particles in the absence of an external magnetic field, sensitive field-induced chain-like aggregation when an external magnetic field is applied, and good recovery of the dispersal after removing the applied magnetic field. From the characteristic contents of both the $\gamma\text{-Fe}_2\text{O}_3$ phase and oleic acid in the composite nanoparticles, as well as the densities of the as-synthesized ferrofluids, the mass fraction percentage ϕ_m , as well as the volume fraction percentage of the magnetic material, i.e., the $\gamma\text{-Fe}_2\text{O}_3$ magnetic core in the composite nanoparticles, ϕ_v , can be obtained. From the relationship between ϕ_v and ϕ_m , ϕ_m can be designed for an acquired ϕ_v in practical applications.

Furthermore, it has been established that the concentration of surfactant controls the growth of nanoparticles upon heating in alkali solution [52]. The present study shows that a high concentration of base may induce a quasi-stability of sizes in the surfactant modification process. This is similar to the preparation of iron oxide nanoparticles in high-pH media [47] and will be studied further.

Funding This study was funded by the Doctoral Foundation of Southwest University (grant number SWU115010) and the Fundamental Research Funds for the Central Universities (grant number XDJK2018B034).

Compliance with ethical standards

Conflict of interest The authors declare that they have no conflict of interest.

Publisher's Note Springer Nature remains neutral with regard to jurisdictional claims in published maps and institutional affiliations.

References

- Jun YW, Seo JW, Chon J (2008) Nanoscaling laws of magnetic nanoparticles and their application in biomedical science. *Acc Chem Res* 41:179–189
- Singamaneni S, Bliznyuk VN, Bineks C, Tymal EY (2011) Magnetic nanoparticles: recent advances in synthesis, self-assembly and application. *J Mater Chem* 21:16819–16845
- Chen F, Smith KA, Hatton TA (2012) A dynamic buildup growth model for magnetic particle accumulation on single wires in high gradient magnetic separation. *AIChE J* 58:2865–2874
- Angelakeris M (2017) Magnetic nanoparticles: a multifunctional vehicle for modern theranostics. *Biochim Biophys Acta* 1861:1642–1651
- Yeom J, Santos US, Chekini M, Cha M, de Moura MF, Kotav NA (2018) Chiro-magnetic nanoparticles and gels. *Science* 359:309–314
- Berkovsky BM, Medvedev VF and Krakov MS (1993) Magnetic fluids engineering application. Oxford Sci Publi, p1
- Sousa MH, Tourinho FA, Depeyrot J, da Silva GJ, Lara MCFL (2001) New electric double-layered magnetic fluids based on copper, nickel, and zinc ferrite nanostructures. *J Phys Chem B* 105:1168–1175
- Holm C, Weis J-J (2005) The structure of ferrofluids: a status report. *Curr Opin Colloid Interface Sci* 10:133–140
- Gautam N, Thirupathi G, Singh R (2016) Magnetoviscosity of paraffin-based barium ferrite ferrofluid. *IEEE Trans Magn* 52:4600204
- Odenbach S (2002) Ferrofluids. Springer-Verlag, Berlin/Heidelberg, p 4
- Dejneka MI, Powell C, Borrelli N, Ouzounov D, Gaeta A (2005) Transparent magnetic glass-ceramics. *J Amer Ceram* 88:2431–2435
- Pu SL, Yao LF, Guan FF, Liu M (2009) Threshold-tunable optical limiters based on nonlinear refraction in ferrosols. *Opt Commun* 282:908–912
- Pop LM, Odenbach S (2006) Investigation of the microscopic reason for the magnetoviscous effect in ferrofluids study by small angle neutron scattering. *J Phys Condens Matter* 18:S2785–S2802
- Buzmakov VM, Pshenichnikov AF (1996) On the structure of microaggregates in magnetite colloids. *J Colloid Interface Sci* 182:63–70
- Taketomi S, Drew RV, Shull RD (2006) Peculiar magnetic after-effect of highly diluted frozen magnetic fluids. *J Magn Magn Mater* 307:77–84
- Lin YQ, Li J, Liu XD, Zhang TZ, Wen BC, Zhang QM, Miao H (2010) Saturation magnetization and law of approach to saturation for self-formed ionic ferrofluids based on MnFe_2O_4 nanoparticles. *Chin J Chem Phys* 23:325–330
- Fosa G, Bădescu R, Călugăru G, Bădescu V (2006) Measuring the transitivity of light: a tool for testing the quality of magnetic liquids. *Opt Mater* 28:461–465
- Baraban L, Erbe A, Leiderer P (2007) Characterization of magnetic colloids by means of magneto-optics. *Eur Phys J E* 23:129–133
- Li J, Zhao BG, Lin YQ, Qiu XY, Ma XJ (2002) Transmission of light in ionic ferrofluid. *J Appl Phys* 92:1128–1131
- Li J, Huang Y, Liu XD, Lin YQ, Li Q, Gao RL (2008) Coordinated chain motion resulting in intensity variation of light transmitted through ferrofluid film. *Phys Lett A* 372:6952–6955
- Mathew DS, Juang R-S (2007) An overview of the structure and magnetism of spinel ferrite nanoparticles and their synthesis in microemulsions. *Chem Eng J* 129:51–65
- Akbarzadem A, Samieí M, Davaran S (2012) Magnetic nanoparticles: preparation, physical properties, and applications in biomedicine. *Nanoscale Res Lett* 7:144
- Bagheri S, Julkapli NM (2016) Modified iron oxide nanomaterials: functionalization and application. *J Magn Magn Mater* 416:117–133
- Chen YS, Chen Q, Mao H, Zhang T, Qiu XY, Lin YQ, Li J (2017) Preparation of magnetic nanoparticles via chemically induced

- transition: dependence of components and magnetization on the concentration of treating solution used. *Nanomater Nanotech* 7:1–9
25. Zhang T, Meng XS, He ZH, Lin YQ, Liu XD, Li DC, Li J, Qiu XY (2017) Preparation of magnetic nanoparticles via a chemically induced transition: role of treating solution's temperature. *Nano* 7:220
 26. Li JM, Li J, Mao H, Lin YQ (2016) Ionic ferrofluids comprising γ -Fe₂O₃ nanoparticles prepared by chemically induced transition: synthesis and magnetization behavior. *J Nanofluids* 5:42–47
 27. Meng XS, He ZH, Zhao JW, Lin YQ, Liu XD, Li DC, Li J, Qiu XY (2018) Oleic acid surface modification in the preparation of magnetic nanoparticles by a chemically induced transition. *IEEE Trans Magn* 54:2300107
 28. Tourinho FA, Franck R, Massart R (1990) Aqueous ferrofluids based on manganese and cobalt ferrites. *J Mater Sci* 25:3249–3254
 29. Wen BC, Li J, Lin YQ, Liu XD, Fu J, Mao H, Zhang QM (2011) A novel preparation method for γ -Fe₂O₃ nanoparticles and their characterization. *Mater Chem Phys* 128:35–38
 30. Sayo T, Iijima T, Soki M, Ingaki N (1987) Magnetic properties of ultrafine ferrite particles. *J Magn Magn Mater* 65:252–256
 31. Sahoo Y, Coodarzo A, Suihart MT, Ohulchanskyy TY, Kaur N, Furlani EP, Prasad PN (2005) Aqueous ferrofluid of magnetite nanoparticles: fluorescence labeling and magnetophoretic control. *J Phys Chem B* 109:3879–3885
 32. Singh M, Ulbrish P, Prokopec V, Svoboda P, Šantavá E, Štěpánek F (2013) Effect of hydrophobic coating on the magnetic and radiofrequency heating of γ -Fe₂O₃ nanoparticles. *J Magn Magn Mater* 339:106–113
 33. Chen M-J, Shen H, Li X, Rnan J, Yuan W-Q (2016) Magnetic fluids' stability improved by oleic acid bilayer-coated structure via one-pot synthesis. *Chem Papers* 70:1642–1648
 34. Liu ZL, Wang HB, Lu QH, Du GH, Peng L, Du YQ, Zhang SM, Yao KL (2004) Synthesis and characterization of ultrafine well-dispersed magnetic nanoparticles. *J Magn Magn Mater* 283:258–262
 35. Berger P, Adelman NB, Beckman KJ, Campell DJ, Ellis AB (1999) Preparation and properties of an aqueous ferrofluid. *J Chem Edu* 76:943–948
 36. Odenbach S (2003) Ferrofluids—magnetically controlled suspensions. *Colloids Surf A Physicochem Eng Asp* 217:171–178
 37. Soares PIP, Laia CAT, Carvalho A, Pereira LCJ, Coutinho JT, Ferreira IMM, Novo CMM, Borges JP (2016) Iron oxide nanoparticles stabilized with a bilayer of oleic acid for magnetic hyperthermia and MRI application. *Appl Surf Sci* 383:240–247
 38. Granqvist CG, Buhman RA (1976) Ultrafine metal particles. *J Appl Phys* 47:2200–2219
 39. Arulmugan R, Naidyanathan G, Sendilnathan S, Jeyadevan B (2005) Co-Zn ferrite nanoparticles for ferrofluid preparation: study on magnetic properties. *Physica B* 363:225–231
 40. Li J, Gong XM, Lin YQ, Liu XD, Chen LL, Li JM, Mao H, Li DC (2014) Investigation into loss in ferrofluid magnetization. *AIP Adv* 4:077123
 41. Taketomi S (2011) Aggregation of magnetic fluids under an external field: micelle formation: a review. *Jourdan J Phys* 4:1–37
 42. Li J, Liu XD, Lin YQ, Huang Y, Bai L (2006) Relaxation behavior measuring of transmitted light through ferrofluids film. *Appl Phys B: Laser Opt* 82:81–84
 43. Huang Y, Li DC, Li F, Zhu QS, Xie Y (2015) Transmitted light relaxation and microstructure evolution of ferrofluids under gradient magnetic field. *Opt Comm* 338:551–559
 44. Shulyma SI, Tanygin BM, Kovalento VF, Petrychuk MV (2016) Magneto-optical extinction trend inversion in ferrofluids. *J Magn Magn Mater* 416:141–149
 45. Li J, Liu XD, Lin YQ, Qiu XY, Ma XJ, Huang Y (2004) Field-induced transmission of light in ionic ferrofluids of tunable viscosity. *J Phys D Appl Phys* 37:3357–3360
 46. Li J, Liu XD, Lin YQ, Bai L, Chen XM, Wang AR (2007) Field modulation of light transmission through ferrofluid film. *Appl Phys Lett* 91:253108
 47. Babes L, Denizot B, Tanguy G, Jeune JLL, Jallet P (1999) Synthesis of iron oxide nanoparticles used as MRI contrast agents: a parametric study. *J Colloid Interface Sci* 212:474–482
 48. Gong XM, Li J, Lin YQ, Liu XD, Chen LL, Li JM, Li DC (2014) Formation of highly crystalline maghemite nanoparticles from ferrihydrite in the liquid phase. *Chin Sci Bull* 59:3904–3911
 49. Taketomia S, Shull RD (2003) Experimental verification of interactions between randomly distributed fine magnetic particles. *J Magn Magn Mater* 266:207–214
 50. Huke B, Lücke M (2004) Magnetic properties of colloidal suspensions of interacting magnetic particles. *Rep Prog Phys* 36:1731–1768
 51. Rosensweig RE (1997) *Ferrohydrodynamics*. Cambridge University Press, P.33
 52. Davis KJ, Wells S, Charles SW (1993) The effect of temperature and oleate adsorption on the growth of maghemite particles. *J Magn Magn Mater* 122:24–28